J Solid State Electrochem (2001) 5: 57–67

ORIGINAL PAPER

A.C. Tavares · M.A.M. Cartaxo
M.I. da Silva Pereira · F.M. Costa

Electrochemical study of spinel oxide systems with nominal compositions $Ni_{1-x}Cu_xCo_2O_4$ and $NiCo_{2-y}Cu_yO_4$

Received: 22 February 1999 / Accepted: 26 October 1999

Abstract Studies on the electrochemical behaviour of $Ni_{1-x}Cu_xCo_2O_4$ ($x \leq 0.75$) and $NiCo_{2-y}Cu_yO_4$ ($y \leq 0.30$) electrodes in 5 mol dm^{-3} KOH aqueous solutions are presented. The oxide layers have been prepared by thermal decomposition of aqueous nitrate solutions on nickel supports at 623 K. Powder samples were also prepared by thermal decomposition under the same conditions. The powder samples and the oxide layers were characterised by X-ray powder diffraction. The influence of the copper content on the voltammetric response of the electrodes and activity towards oxygen evolution reaction is analysed and correlated with the surface composition of the electrodes by means of X-ray photoelectron spectroscopy data. The analysis of the results reveals that the presence of Cu affects the electrode behaviour and its influence depends on which cation has been replaced.

Key words Ni-Co-Cu spinel oxides · Thermal decomposition · X-ray diffraction · X-ray photoelectron spectroscopy · Cyclic voltammetry

Introduction

Cyclic voltammetry of $NiCo_2O_4$ electrodes in alkaline solutions yields a well-known pattern due to the redox processes involving both nickel and cobalt ions [1, 2]. However, when the partial replacement of one of these cations in the spinel structure is performed, modifications to the voltammetric pattern are observed, particularly in the cathodic sweep [3–5].

In previous work the partial replacement of cobalt by rhodium has been attempted, leading to spinel oxides of nominal composition $NiCo_{2-x}Rh_xO_4$ ($0.0 \leq x \leq 0.5$) [4]. The choice of rhodium was due to the high stability of Rh^{3+}, in addition to its preference to occupy the octahedral sites in the spinel structure [6]. The electrodes prepared by thermal decomposition at 350 °C have low crystallinity, leading to very difficult structural characterisation. Electrodes prepared at higher temperatures allow better structural characterisation and led us to correlate structure/composition/activity. These studies have shown that Rh clearly contributes to an increase of the electrode surface area but has no appreciable influence on the oxygen evolution mechanism.

In order to explore these correlations, studies on the effect of the partial replacement of nickel by copper in the $NiCo_2O_4$ electrodes were performed by X-ray photoelectron spectroscopy (XPS) and cyclic voltammetry [3]. The electrodes were prepared by thermal decomposition on a nickel mesh using the dipping method. Cu(II) substitutes Ni(II) very easily [6], leading to the formation of single-phase oxides of nominal composition $Ni_{1-x}Cu_xCo_2O_4$ ($0.00 \leq x \leq 0.75$) at low preparation temperatures. Moreover, thermodynamic data predict that copper species do not undergo redox processes in the potential range where cobalt and nickel species do. XPS data show that the copper introduction leads to significant modifications of the electrode surface composition, being the surface layers mainly formed by a rich nickel-copper spinel phase. This effect could also be followed by cyclic voltammetry. Studies on electrode activity towards the oxygen evolution reaction (OER) have been performed and a direct relation with the Ni(II) species surface concentration was observed [7].

Other preparation procedures were tested to prepare $NiCo_2O_4$ electrodes, taken as the standard electrode. It was found that a richer surface in nickel was obtained when a nickel foil substrate was used and the brush painting method applied [7].

A.C. Tavares[1] · M.A.M. Cartaxo
M.I. da Silva Pereira (✉) · F.M. Costa
CITECMAT, Departamento de Química e Bioquímica da Faculdade de Ciências de Lisboa, Campo Grande, 1700 Lisboa, Portugal
e-mail: misp@fc.ul.pt; Fax: +351-1-7599404

Present address:
[1] Department of Physical Chemistry and Electrochemistry, University of Milan, Via Venezian 21, 20133 Milan, Italy

The replacement of cobalt by copper was then attempted and a series of new oxide electrodes with nominal composition $NiCo_{2-y}Cu_yO_4$ ($0.00 \le y \le 0.30$) was prepared using the brush painting method and a nickel foil substrate [7]. Also for this system the electrodes' surface composition is strongly affected by copper introduction in the oxide structure. The effect of composition on electrode activity towards the OER has been performed and a direct relationship with the Ni(II) species surface concentration was also observed [7].

In this work the role of the copper(II) ions in the spinel structure is investigated and its effect on the electrochemical behaviour of the cobalt-nickel based spinel oxides, with nominal composition $NiCo_{2-y}Cu_yO_4$ ($0.00 \le y \le 0.30$) and $Ni_{1-x}Cu_xCo_2O_4$ ($0.00 \le x \le 0.75$), is considered. Structural characterisation of both systems was performed through X-ray diffraction (XRD) analysis.

For each oxide system, the influence of the amount of copper on the voltammetric behaviour and electrocatalytic activity is analysed by comparison with that of $NiCo_2O_4$ electrodes prepared by the same procedure.

XPS data are used to obtain detailed information on the electrode surface composition and are correlated to the oxide electrochemical behaviour and activity for the OER.

Experimental

Preparation of samples

Two types of oxide samples were prepared: powders and electrodes. The powders were prepared by thermal decomposition of aqueous solutions containing the corresponding nitrates [1 mol dm^{-3} $Ni(NO_3)_2 \cdot 6H_2O$, 2 mol dm^{-3} $Co(NO_3)_2 \cdot 6H_2O$, 1 mol dm^{-3} $Cu(NO_3)_2 \cdot 6H_2O$ Merck], mixed in stoichiometric amounts according to the required final nominal composition. The powders obtained were then treated at 623 K in air for 1 h. The nominal compositions studied are $x = 0.00$, 0.05, 0.10, 0.25, 0.50, 0.75, 1.00 for the $Ni_{1-x}Cu_xCo_2O_4$ system and $y = 0.00$, 0.05, 0.10, 0.20, 0.30, 0.50 for the $NiCo_{2-y}Cu_yO_4$ system.

The electrodes were prepared by coating nickel supports (typically 0.3×0.5 cm^2) with successive layers of the oxides obtained by thermal decomposition in the same conditions as the powder samples. Slightly different procedures were used for the electrode's preparation [7]. The electrodes with nominal composition $Ni_{1-x}Cu_xCo_2O_4$ were prepared by dipping the pre-treated nickel mesh into the nitrates solution and those with nominal composition $NiCo_{2-y}Cu_yO_4$ by brushing the aqueous nitrates solution onto the pre-treated nickel foil support. The electrodes were then annealed at 623 K for 1 h. The oxide loading varies from 8 to 10 mg cm^{-2}. The details of the preparation can be found in a previous paper [8]. The nominal compositions studied are $x = 0.00$, 0.05, 0.10, 0.25, 0.50, 0.75 for the $Ni_{1-x}Cu_xCo_2O_4$ system and $y = 0.00$, 0.05, 0.10, 0.20, 0.30 for the $NiCo_{2-y}Cu_yO_4$ system.

XRD studies

Powder samples and oxide layers (scraped from the nickel supports and ground in an agate mortar) were characterised by XRD, using a Philips PW 1730 X-ray diffratometer with automatic data acquisition [APD Phillips (v.35B) software]. All scans were recorded between 10° and 80° 2θ at a scanning rate of 0.02° s^{-1}, using Cu K_α radiation ($\lambda = 0.15406$ nm) as the incident radiation.

XPS studies

The XPS analysis was performed using an ESCALAB 200A (VG Scientific) surface analysis instrument, operating under VG5250 data acquisition and analysis software. For surface excitation an achromatic, Mg anode X-ray source, operating at 15 eV (300 W), was used. Spectrometer calibration was done with reference to Ag $3d_{5/2}$ (368.27 eV) on a clean Ar^+ ion-etched Ag sample. The base pressure inside the spectrometer during analysis was better than 10^{-6} Pa and spectrum data were acquired with 20 eV CAE pass energy.

For spectral analysis, the facilities available on the VG5250 Data Analysis were used, namely non-linear Shirley-type background subtraction and peak fitting using a mixed Gaussian-Lorentzian peak function (with G/L ratio optimised by the program) [9]. Quantitative analysis was based on peak area intensity measurement corrected using the Scofield photoionisation cross-sections and spectrometer transfer function (VG-ESCALAB), as available in the system procedures for quantitative analysis [10].

Electrochemical studies

The electrochemical experiments were performed in a three-compartment glass cell at room temperature, using a 5 mol dm^{-3} KOH (Merck) as electrolyte solution. As counter electrode a platinum foil was used and as reference a Hg/HgO electrode.

The electrochemical measurements were carried out using a low-noise operational amplifier potentiostat incorporated with a positive feedback iR compensation, programmed by a Hi-Tec PPRI waveform generator and a Philips 8271 *x-y-t* recorder.

Steady state measurements were performed after stabilising the electrode at the highest potential for 20 min, in order to obtain a stable surface. The steady state currents were recorded in the direction of decreasing potential.

Results and discussion

Structural characterization and surface analysis

XRD studies

X-ray diffractograms of both $Ni_{1-x}Cu_xCo_2O_4$ and $NiCo_{2-y}Cu_yO_4$ powder samples were recorded. In all diffractograms the characteristic lines of a cubic spinel structure like $NiCo_2O_4$ [11] are present, but extra lines were also detected for samples with nominal compositions $CuCo_2O_4$ and $NiCo_{1.5}Cu_{0.5}O_4$.

Figures 1 and 2 present the X-ray diffractograms for three powder samples belonging to the $Ni_{1-x}Cu_xCo_2O_4$ and $NiCo_{2-y}Cu_yO_4$ systems, respectively. The diffractograms shown correspond to (a) a $NiCo_2O_4$ sample, (b) the limiting nominal compositions where only the spinel diffraction lines are present ($x = 0.75$ and $y = 0.30$), and (c) the next prepared composition where the extra diffraction lines were detected ($x = 1.00$ and $y = 0.50$). The second phase, when formed, is the CuO [12] in the case of the $Ni_{1-x}Cu_xCo_2O_4$ system and the NiO [13] in the case of the $NiCo_{2-y}Cu_yO_4$ system.

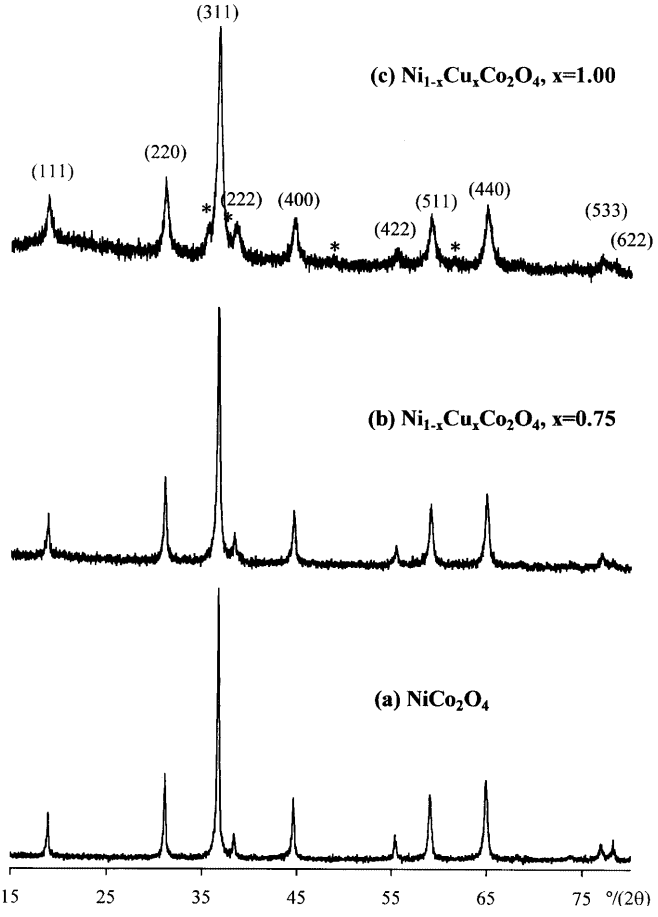

Fig. 1 X-ray diffractograms for the $Ni_{1-x}Cu_xCo_2O_4$ powder samples with **a** $x = 0.00$, **b** $x = 0.75$ and **c** $x = 1.00$. Peaks of the second phase formed are indicated by an *asterisk*

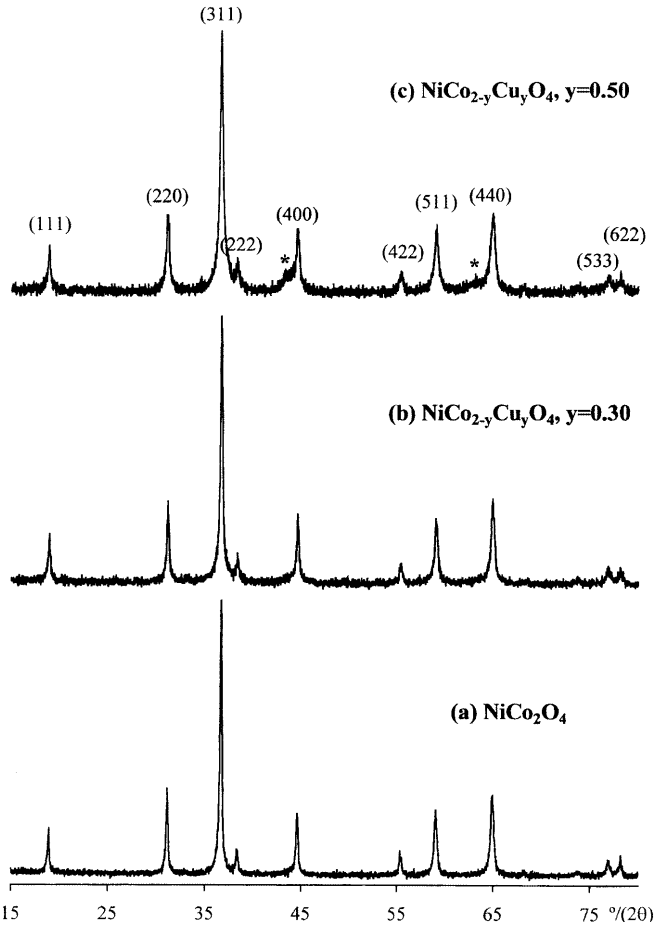

Fig. 2 X-ray diffractograms for the $NiCo_{2-y}Cu_yO_4$ powder samples with **a** $y = 0.00$, **b** $y = 0.30$ and **c** $y = 0.50$. Peaks of the second phase formed are indicated by an *asterisk*

As expected, the samples crystallinity is low owing to the preparation conditions to obtain samples with a high surface area, and decreases significantly with the addition of copper.

The electrodes were prepared just for the nominal compositions where only a single phase is formed and X-ray diffractograms of the oxide layers were also recorded for each composition. The diffractograms of the scraped layers have the same pattern as the powder samples but with a much lower degree of crystallinity, particulary for the $NiCo_{2-y}Cu_yO_4$ system [7, 14].

Tables 1 and 2 present the cell parameter values for the cubic spinel phase calculated considering the JCPDS data file for the $NiCo_2O_4$ spinel structure [11] and using the LSUCRE software for X-ray data indexation and refinement [15].

For the $NiCo_2O_4$ powder samples the cell size value is close to 0.811 nm, which is in good agreement with the one reported in the JCPDS data file [11]. However, for the scraped layers a slightly higher value was obtained, which should reflect the influence of the nickel support. The metallic support in contact with the reactants favours the presence of the cations in the lowest oxidation states, which in consequence leads to an increase of the cell size.

When copper ions are introduced in the spinel structure, an increase of the cell size occurs for both systems. This increment is smaller for all powder samples and for the $Ni_{1-x}Cu_xCo_2O_4$ scraped layers than for the $NiCo_{2-y}Cu_yO_4$ scraped layers.

The different limiting values for the formation of the solid solution, $x = 0.75$ and $y = 0.30$ for the $Ni_{1-x}Cu_xCo_2O_4$ and $NiCo_{2-y}Cu_yO_4$ systems respectively, should reflect important differences between the cationic rearrangement in the two systems.

Table 1 Cell parameter values, a, for the cubic spinel phase as a function of copper content for the $Ni_{1-x}Cu_xCo_2O_4$ powder and scraped layer samples

x	a (nm)	
	Powder	Scraped layer
0.00	0.8105(1)	0.8112(2)
0.05	0.8111(2)	0.8111(3)
0.10	0.8112(1)	0.8112(2)
0.25	0.8112(2)	0.8116(1)
0.50	0.8110(2)	0.8107(2)
0.75	0.8115(1)	0.8115(3)
1.00	0.8113(2)	–

Table 2 Cell parameter values, a, for the cubic spinel phase as a function of copper content for the $NiCo_{2-y}Cu_yO_4$ powder and scraped layer samples

y	a (nm)	
	Powders	Scraped layer
0.00	0.8105(1)	0.8111(2)
0.05	0.8111(1)	0.8111(3)
0.10	0.8110(2)	0.8118(4)
0.20	0.8110(3)	0.8119(3)
0.30	0.8113(2)	0.8118(3)
0.50	0.8118(1)	–

XPS studies

All oxide layers were investigated by means of XPS analysis. Survey spectra and core level spectra [C(1s), O(1s) and M($2p_{3/2}$)] were recorded. The survey spectra show that, except for carbon, all electrode surfaces are free from any contamination.

The detailed XPS analysis of both Cu-containing oxide system, has been previously reported [3, 7] and in this paper is only briefly reviewed. A representative set of the recorded and resolved O(1s) and M($2p_{3/2}$) core level spectra for an electrode with $x = 0.50$ ($Ni_{0.5}Cu_{0.5}Co_2O_4$) is shown in Fig. 3. Table 3 summarises the peak parameter values, which characterise the resolved spectra shown in Fig. 3, as well as the possible species, which is responsible for the features in each spectrum.

Two kinds of nickel species have been detected and assigned to species containing Ni(II) and Ni(III) ions. The Ni(III)/Ni(II) ratio decreases in both systems with the amount of copper, but with different trends [3, 7]. Copper(II) ions were detected in both tetrahedral and octahedral coordinations and Table 4 presents the amount of Cu(II) species in each coordination for the two oxide systems. Figure 4 contrasts the values of the $Cu(II)_{oct}/Cu(II)_{tet}$ atomic ratio for the two systems. It is almost constant and equal to one for the $NiCo_{2-y}Cu_yO_4$ system while for $Ni_{1-x}Cu_xCo_2O_4$ it shows a clear dependence on x.

The XPS data show that the electrode surface composition is significantly affected by the presence of

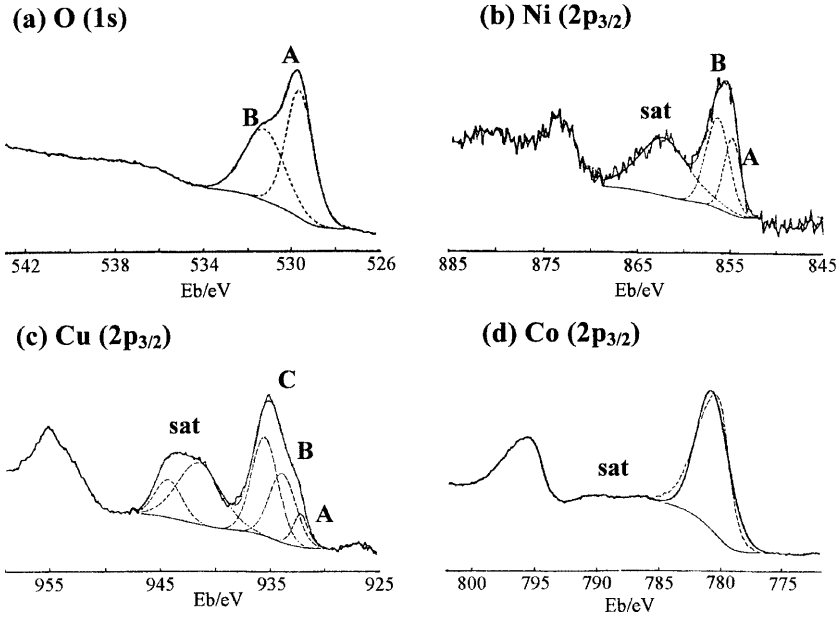

Fig. 3 Recorded and resolved core level spectra for a $Ni_{1-x}Cu_xCo_2O_4$ electrode with $x = 0.50$; **a** O (1s), **b** Ni ($2p_{3/2}$), **c** Cu ($2p_{3/2}$) and **d** Co ($2p_{3/2}$)

Table 3 Binding energies, E_b, FWHM and G/L values obtained for the resolved core level spectra for a $Ni_{1-x}Cu_xCo_2O_4$ electrode with $x = 0.50$

Line	Peak	Species	E_b (eV)	FWHM (eV)	G/L (%)	Ref.
O(1s)	A	Lattice O^{2-} ions	529.6	1.5	42	[16]
	B	adsorbed O-containing species (OH,....)	531.2	2.3	31	
Ni($2p_{3/2}$)	A	Ni(II) ions (as in NiO)	854.6	2.0	56	[3, 17–22]
	B	Ni(III) ions [or Ni(II) ions as in $Ni(OH)_2$]	856.0	3.4	24	
	satellite	paramagnetic Ni(II)/Ni(III) ions	862.4	6.8	11	
Co($2p_{3/2}$)	A	mainly Co(III) ions	780.6	3.1	8	[23]
Cu(2p3/2)	A	Cu(I) ions (tetrahedral coordination)	932.4	1.6	18	[18, 19, 24]
	B	Cu(II) ions in octahedral coordination	934.6	2.9	14	
	C	Cu(II) ions in tetrahedral coordination	936.2	2.9	33	
	sat. I	paramagnetic Cu(II) ions	941.2	4.0	54	
	sat. II	paramagnetic Cu(II) ions	944.1	3.2	4	

Table 4 XPS speciation of Cu ions for the $NiCo_{2-y}Cu_yO_4$ and $Ni_{1-x}Cu_xCo_2O_4$ electrodes

x	Peak area (%)			y	Peak area (%)		
	Cu-A	Cu-B	Cu-C		Cu-A	Cu-B	Cu-C
0.05	8	32	19	0.05	1	23	40
0.10	9	21	27	0.10	7	22	30
0.25	9	12	12	0.20	3	25	31
0.50	8	35	15	0.30	3	27	31
0.75	8	43	8				

copper. A surface enrichment in copper is found for all the electrodes studied, which can be seen clearly in Fig. 5, where the dependence of the Cu/Co atomic ratio on the nominal copper content (x, y) for $Ni_{1-x}Cu_xCo_2O_4$ and $NiCo_{2-y}Cu_yO_4$ electrodes is presented. The lines inferred from the nominal composition of the oxides are also included in the figure.

XPS analysis also indicates a strong dependence of the Ni/Co atomic ratio on the nominal copper content. Earlier results showed that electrode surfaces more rich in nickel are obtained when nickel foil/brush painting is applied [7], as Table 5 illustrates for the $NiCo_2O_4$ electrodes prepared by the two different procedures reported in this work. In order to eliminate the effect of different preparation conditions on the analysis, the Ni/Co atomic ratio value obtained for each copper-containing electrode was divided by the average value of the $NiCo_2O_4$ electrodes prepared under the same conditions. The values obtained are presented in Fig. 6, and show that the atomic ratio is a maximum for $x = 0.10$ and $y = 0.30$ and a minimum for $y = 0.10$.

Correlation between XRD and XPS results

For the $NiCo_2O_4$ spinel oxide electrodes, several cationic distributions have been proposed based on X-ray and neutron diffraction studies, magnetic susceptibility measurements, XPS analysis, etc. [25–28]. However, since the $NiCo_2O_4$ electrodes are normally prepared by thermal decomposition at low temperatures, and with short thermal treatment, the samples crystallinity is not very high and so it is difficult to propose a precise cationic distribution along the spinel structure.

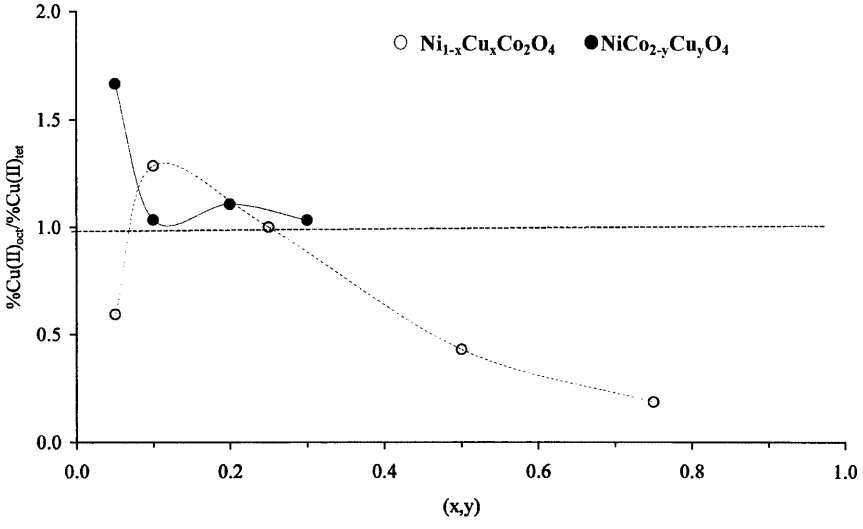

Fig. 4 Variation of the $Cu(II)_{oct}/Cu(II)_{tet}$ atomic ratio determined by XPS as a function of the nominal copper content (x or y) for the $Ni_{1-x}Cu_xCo_2O_4$ and $NiCo_{2-y}Cu_yO_4$ electrodes

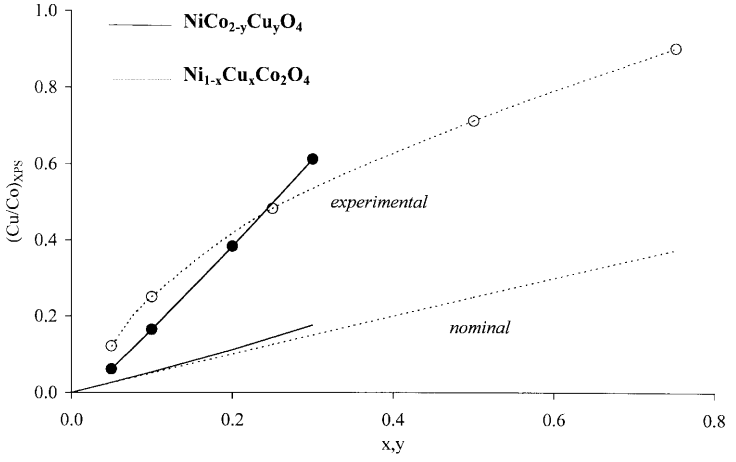

Fig. 5 Variation of the $(Cu/Co)_{XPS}$ atomic ratio determined by XPS as function of the nominal copper content (x or y) for the $Ni_{1-x}Cu_xCo_2O_4$ and $NiCo_{2-y}Cu_yO_4$ electrodes. The nominal dependence is also shown

Table 5 Ni/Co atomic ratio for the $NiCo_2O_4$ electrodes prepared by different procedures

Preparation procedure	Ni/Co atomic ratio
Nickel foil/brush painting	1.1
Nickel mesh/dipping	0.8

For a qualitative discussion of the X-ray diffraction data we will assume a general cationic distribution for the $NiCo_2O_4$ spinel oxide, like:

$$Co^{2+}_{1-a}Co^{3+}_{a}[Ni^{2+}_{b}Ni^{3+}_{1-b}Co^{3+}]O^{2-}_{4-z}$$

with $z = (a-b)/2$ proposed by Hanen et al. [25] for oxides prepared in a similar way to those reported in this work. Owing to the reactants nature, preparation method and conditions, the copper should enter in the spinel structure as Cu^{2+} ions. According to the excess octahedral stabilisation energy values for these ions [29], they should occupy preferentially the octahedral sites in the spinel structure. Because the ionic radius of Cu^{2+} ions in ocathedral coordination is higher than those of Ni^{2+}, Ni^{3+} or Co^{3+} (ions in the same coordination) [6], a progressive increase of the cell size with copper introduction is expected for both systems.

Studies on several copper-containing spinels [5, 30–33] have shown that Cu(II) ions tend to occupy simultaneously both sites of the spinel structure, and the same feature was observed in our systems [3, 7].

For the $Ni_{1-x}Cu_xCo_2O_4$ system the presence of Cu^{2+} ions in the tetrahedral sites means that part of the Co^{2+} ions moved from the tetrahedral sites to the octahedral ones, giving rise to an increase of octahedral Co^{3+} ion content. The Co^{3+} ions will occupy the free places left by the nickel ions, and the final charge balance is achieved by either decreasing the Ni^{3+} content and/or changing the oxygen stoichiometry.

For the $NiCo_{2-y}Cu_yO_4$ system, the picture is much more complex. First of all it should be noted that we were able to replace only 30% of cobalt with copper. XPS also detected the presence of Cu^{2+} ions in both sites of the spinel structure. If Cu^{2+} ions are present in the octahedral sites and if they are going to replace Co^{3+} ions, there will be a net defficiency of positive charges. This means that the presence of Cu^{2+} ions is tolerated only for small amounts, in this case for $y \leq 0.30$, and in fact XPS data showed that an oxygen deficiency occurs [7]. For higher copper content, the Ni^{2+} ions leave the spinel structure in order to avoid the charge balance problem.

Electrochemical studies

Voltammetric studies

The effect of composition on the voltammetric behaviour of cobalt-nickel based spinel oxides is clearly seen in Fig. 7, which presents stabilised responses of fresh $Ni_{1-x}Cu_xCo_2O_4$ and $NiCo_{2-y}Cu_yO_4$ electrodes of selected nominal compositions in 5 mol dm^{-3} KOH. As reference, a cyclic voltammogram of a fresh $NiCo_2O_4$ electrode (nickel mesh/dipping) is also included.

According to thermodynamic data, copper species do not suffer redox processes in the potential region under study [34], and experimental results reported for copper-containing spinel oxides have confirmed this [35, 36]. It is therefore clear that the different behaviour shown by the two systems reflects differences in the compositional/cationic distribution of the oxides, induced by the copper ions.

The set of redox peaks A_I/C_I and A_{II}/C_{II}, usually observed in the voltammetric response of $NiCo_2O_4$ electrodes in alkaline solutions, has already been discussed in detail in many papers and their assignment proposed by many authors [1–3]. Table 6 summarises the peak assignments.

The Cu-containing oxides show anodic profiles similar to those for $NiCo_2O_4$, although variations in the current density of peaks A_I and A_{II} are observed for all samples and a shift of peak A_{II} to more positive potentials is clearly seen for the $Ni_{1-x}Cu_xCo_2O_4$ system when $x > 0.25$.

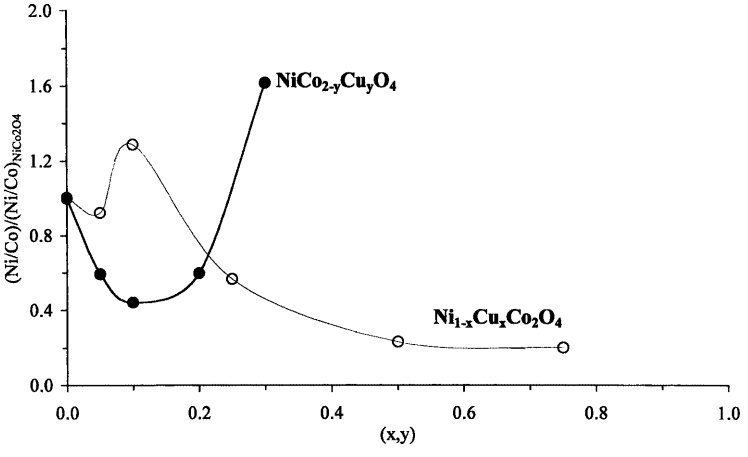

Fig. 6 Dependence of the $(Ni/Co)/(Ni/Co)_{NiCo_2O_4}$ atomic ratio determined by XPS on the nominal copper content (x or y) for the $Ni_{1-x}Cu_xCo_2O_4$ and $NiCo_{2-y}Cu_yO_4$ electrodes

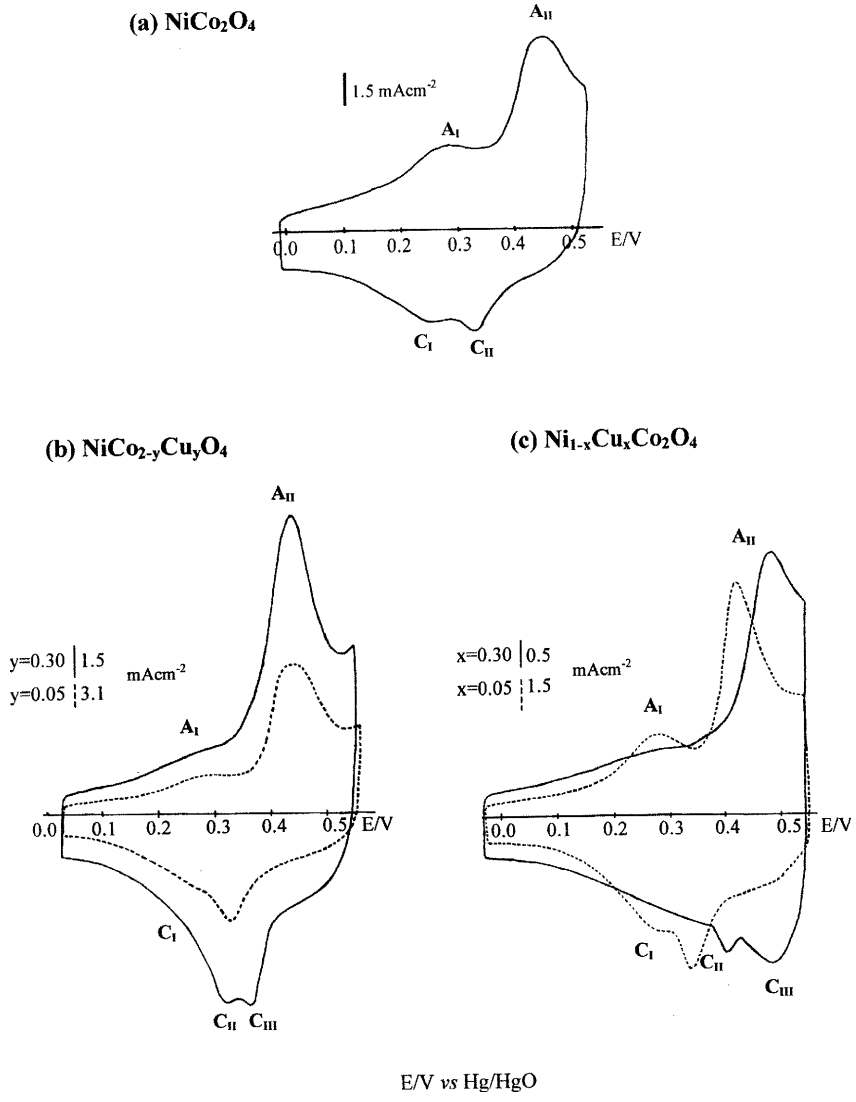

Fig. 7 Cyclic voltammograms for the oxide electrodes: **a** $NiCo_2O_4$, **b** $NiCo_{2-y}Cu_aO_4$ with $y = 0.05$ (*broken line*) and 0.30 (*full line*), and **c** $Ni_{1-x}Cu_xCo_2O_4$ with $x = 0.05$ (*broken line*) and $x = 0.75$ (*full line*), obtained in 5 mol dm^{-3} KOH at a sweep rate of 10 mV s^{-1}

To eliminate the effect of using different preparation procedures, the anodic peak current density obtained for each copper-containing electrode was divided by the average value obtained for the $NiCo_2O_4$ electrodes, prepared by the same procedure. Figure 8a and b shows the variation in the peak current density ratio $j/j\,NiCo_2O_4$ with the nominal amount of copper. Concerning peak A_I, a similar variation is observed for both systems, showing a maximum value at $y = x = 0.10$, followed by a decrease in the current density due to the decrease in the quantity of Co(II) ions in tetrahedral sites. These variations reflect the changes in the Co(II)/Co(III) ratio, which we were not able to follow by XPS studies [3, 7]. It should be mentioned here that, for the $Ni_{1-x}Cu_xCo_2O_4$ system, a decrease in the Co(II) ion content means an increase in Co(III) ion content in octahedral sites, once the amount of cobalt has been kept constant.

For the $NiCo_2O_4$ oxide electrodes, peak A_{II} is mainly caused by the oxidation of Co(III), being the Co(III) species both originally present in the octahedral sites and those formed in A_I, with a minor contribution from the oxidation of Ni(II) ions [3, 25]. The maximum observed for both systems when $x = y = 0.10$ reflects the variation in the current density of peak A_I. The current increase for the samples with x, $y > 0.20$ is due to the increase of the relative amounts of Ni(II) and Co(III) species for the system $Ni_{1-x}Cu_xCo_2O_4$ and of Ni(II) species for the system $NiCo_{2-y}Cu_yO_4$ on the electrode surface. This explanation is consistent with the variation of the peak current ratio, $j_{A_{II}}/j_{A_I}$, with the nominal amount of copper in the electrodes, presented in Fig. 8c.

Table 6 Assignment of the processes involved in the voltammetric peaks for $NiCo_2O_4$ electrodes [1, 2]

Peaks	Peak assignement
A_I/C_I	$Co(II)_{tet} \rightleftharpoons Co(III)_{tet} + e^-$
A_{II}/C_{II}	$Co(III)_{tet} + Co(III)_{Oct} \rightleftharpoons Co(IV) + 2e^-$ [a]
	$Ni(II) \rightleftharpoons Ni(III) + e^-$

[a] Dominant process

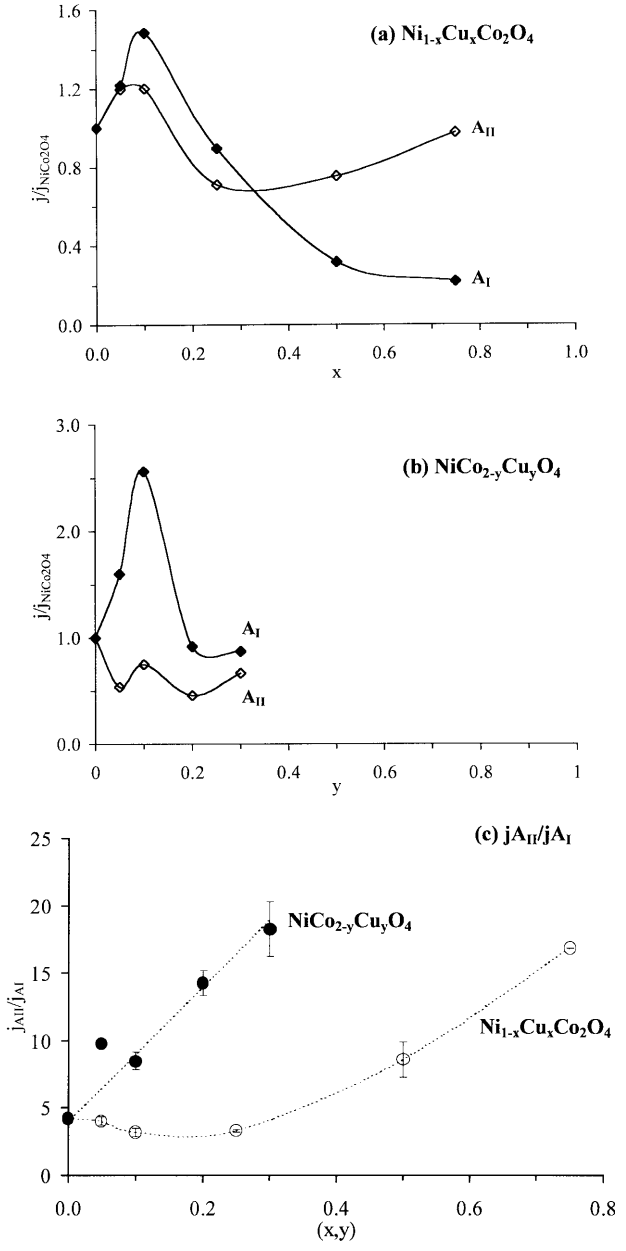

Fig. 8 Variation of the intensity ratio between the anodic peak current density for the copper containing electrodes and the corresponding value for the $NiCo_2O_4$ electrodes prepared by the same procedure, with the nominal amount of copper (x or y) for the oxide systems **a** $Ni_{1-x}Cu_xCo_2O_4$ and **b** $NiCo_{2-y}Cu_yO_4$, **c** intensity peak ratio ($j_{A_{II}}/j_{A_I}$) vs. the nominal amount of copper x or y

These observations are in accordance with earlier results obtained in our laboratory for $NiCo_{2-x}Rh_xO_4$ electrodes [4]. Indeed, no significative changes in peak A_I were observed with the progressive increase of rhodium content, as was expected once Rh^{3+} is replacing the Co^{3+} in the octahedral sites according to its site preference.

On the return scan, systematic variations in the voltammetric response result from the presence of copper. For the $Ni_{1-x}Cu_xCo_2O_4$ system peaks C_I and C_{II} are displaced and the appearance of a third peak, C_{III}, between 0.42 and 0.49 V occurs when $x \geq 0.50$. For the $NiCo_{2-y}Cu_yO_4$ system no appreciable shift of peaks C_I and C_{II} is observed and peak C_{III} is formed between 0.35 and 0.40 V, when $y \geq 0.20$. Studies on the influence of the positive potential limit on the electrode voltammetric behaviour show that peak C_{III} is related to the anodic peak A_{II} [3].

The study of the effect of sweep rate on the voltammetric response indicates that, for each composition, the peak current varies with sweep rate according to $I_p \propto v^{0.8}$ and no appreciable shift of the peak potential was observed with increasing sweep rate.

In a previous paper concerning the $Ni_{1-x}Cu_xCo_2O_4$ system, the authors assigned peaks A_{II}/C_{III} to the redox couple Ni(III)/Ni(II) [3]. Regarding the oxide system with nominal composition $NiCo_{2-y}Cu_yO_4$, the same assignment is made, although the A_{II}/C_{III} pair of peaks appears at a different potential. This assignment was based on both the inactivity of copper ions in this potential region and the increase of the amount of Ni(II) ions revealed by the XPS studies. The difference in potential comes from the independence of the anodic peak A_{II}, on the copper content on the bulk/surface of the $NiCo_{2-y}Cu_yO_4$ electrodes.

These results show that copper introduction in the $NiCo_2O_4$ lattice contributes to the resolution of peak C_{II} usually attributed to the reduction process involving both Co(IV)/Co(III) and Ni(III)/Ni(II) redox couples.

Considering the voltammetric response of the two samples with the highest amount of copper, it is evident that the effect of the presence of copper is more visible for $Ni_{1-x}Cu_xCo_2O_4$ than on the $NiCo_{2-y}Cu_yO_4$. This behaviour could be explained by a perturbation effect of the copper ions on the $NiCo_2O_4$ lattice that is more explicit for the $Ni_{1-x}Cu_xCo_2O_4$ system due to the larger amount of copper introduced.

Figure 9 presents the dependence on the nominal copper amount of the ratio between the total voltammetric charge density obtained by integration of the voltammetric curves for each copper-containing electrode and the corresponding average value obtained for the $NiCo_2O_4$ electrodes prepared by the same procedure. A decrease in the charge densities is expected, owing to the copper inactivity in the potential region under study.

Indeed, the $NiCo_{2-y}Cu_yO_4$ system shows the expected behaviour in the whole composition range studied. Contrarily, the $Ni_{1-x}Cu_xCo_2O_4$ system exhibits a well-defined maximum between $x = 0.05$ and 0.10. This behaviour reflects the surface enrichment in nickel species and Co(II) when $x \leq 0.10$, demonstrated by the XPS data analysis and cyclic voltammetry, respectively [3].

Electrocatalytic activity towards OER

Catalysed oxygen evolution is highly sensitive to the nature and structure of the electrode surface [37]. Cor-

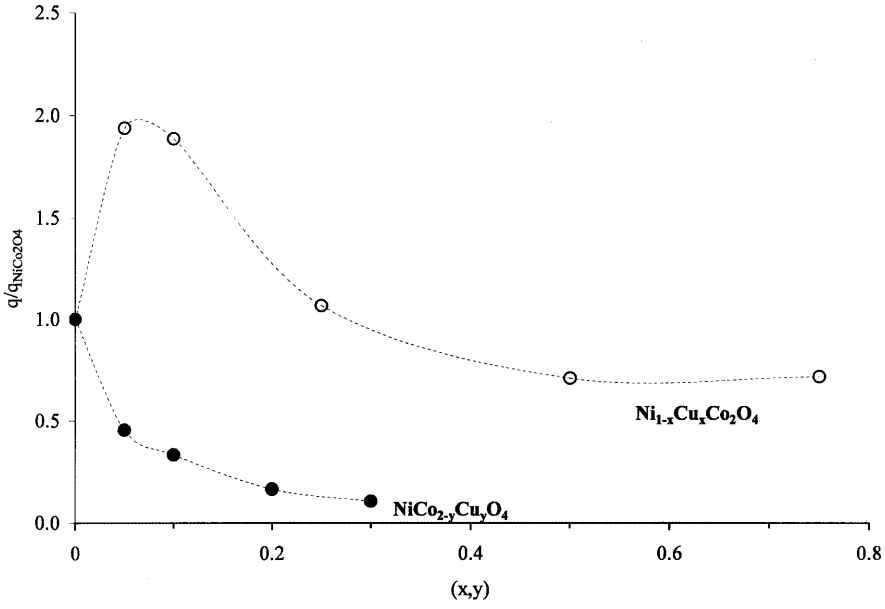

Fig. 9 Dependence of the ratio between the voltammetric charge density for the copper-containing electrodes and the corresponding value for the $NiCo_2O_4$ electrodes prepared by the same procedure on the nominal copper content (x, y) for the ○ $Ni_{1-x}Cu_xCo_2O_4$ and ● $NiCo_{2-y}Cu_yO_4$ electrodes

respondingly, the presence of copper in the nickel and cobalt spinel oxide should affect the electrochemical activity of the electrodes towards the OER and a different behaviour is indeed observed, depending on which cation is replaced by copper, as earlier reported [7].

In a previous paper we have analysed the Tafel lines for the two copper-containing spinel oxide systems, taking into account the electrode roughness [7]. It has been concluded that there is a correlation between the electrode activity for the OER and its surface composition and a direct relationship could be found between the amount of nickel, in particular the % of Ni(II) ions on the electrodes surface, and its activity. The electrodes with higher activity are those with a less oxidised surface, rich in nickel, and showing a higher concentration of Ni(II) ions.

Figure 10 shows two representative apparent current density-potential curves for oxygen evolution (current normalised for the electrodes geometric area) and

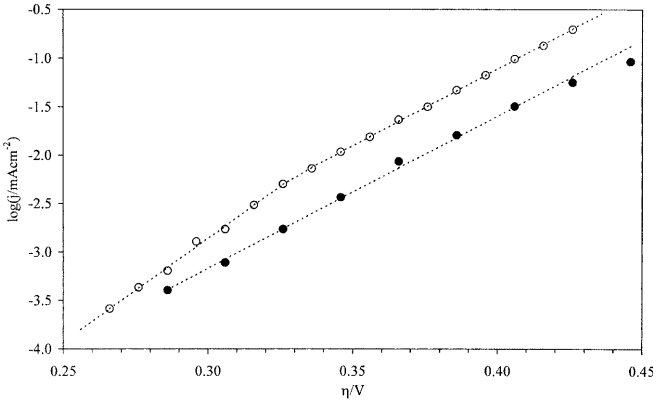

Fig. 10 Tafel plots for oxygen evolution on ○ $Ni_{1-x}Cu_xCo_2O_4$ and ● $NiCo_{2-y}Cu_yO_4$ electrodes with $x = y = 0.10$ in 5 mol dm^{-3} KOH. Current normalised considering the geometric area

Table 7 summarises the values earlier reported for the Tafel slopes for the two oxide systems, $Ni_{1-x}Cu_xCo_2O_4$ and $NiCo_{2-y}Cu_yO_4$ [7]. The values are in accordance with those usually reported for the nickel-cobalt based spinel oxide electrodes. Different values ranging from 40 to 120 mV have been reported in the literature, depending upon the method of preparation of the oxides, the nature of the substrate and the experimental conditions [4, 35, 36, 38–40].

In this work the electrocatalytic activity (including electronic and geometric factors) of the two systems is evaluated in terms of overpotential measured at a current density selected on the basis of a constant value of the Tafel slope for all the samples (60 mV). The dependence of the overpotential for oxygen evolution, measured at an apparent current density of 10 mA cm^{-2}, on the nominal amount of Cu in the samples is presented in Fig. 11. In general, the overpotential is lower for the electrodes with nominal composition $NiCo_{2-y}Cu_yO_4$, excluding the sample with $y = 0.10$, which is associated with the higher amount of nickel in the samples. Moreover, within this system, and once again excluding the sample with $y = 0.10$, the overpotential dependence on the nominal composition follows the trend expected from the voltammetric charge variation.

Table 7 Electrode kinetics parameters for oxygen evolution on $NiCo_{2-y}Cu_yO_4$ and $Ni_{1-x}Cu_xCo_2O_4$ electrodes

System	Copper amount (x, y)	Tafel slope (mV)	
		Low current density	High current density
$Ni_{1-x}Cu_xCo_2O_4$	$x \leq 0.25$	45 ± 3	62 ± 4
	$x \geq 0.50$	60 ± 4	
$NiCo_{2-y}Cu_yO_4$	$y \neq 0.10$	64 ± 10	108 ± 20
	$y = 0.10$	60 ± 10	

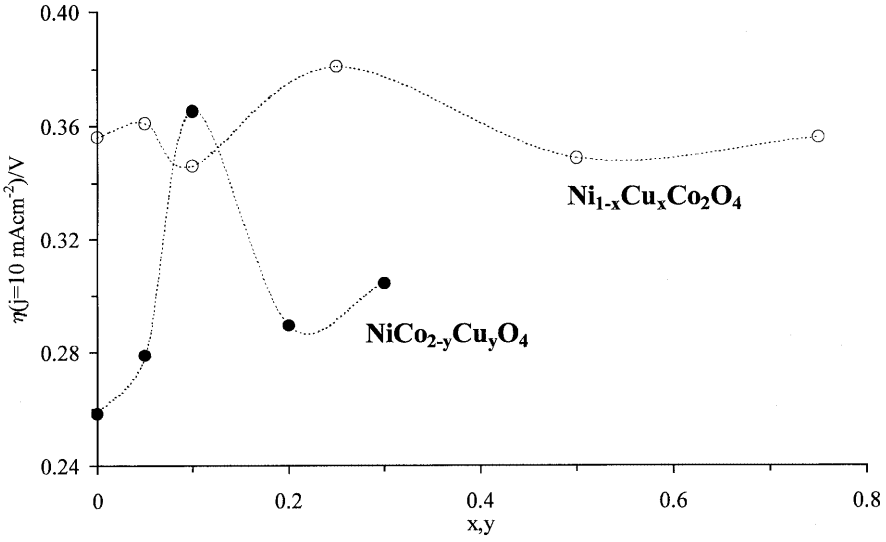

Fig. 11 Dependence of the oxygen evolution overpotential on the nominal copper content (x, y) for $Ni_{1-x}Cu_xCo_2O_4$ and $NiCo_{2-y}Cu_yO_4$ electrodes in 5 mol dm^{-3} KOH, at a current density of 10 mA cm^{-2} normalised for the geometric area

Concerning the system $Ni_{1-x}Cu_xCo_2O_4$, the general trend is similar to that observed for the atomic ratio $(Ni/Co)_{XPS}$ vs. x, y, the nominal amount of copper in the samples.

It is clear that the balance of two aspects, the real surface area and the surface composition of the electrodes, determine the observed behaviour, and its influence depends on the specific system. For the $Ni_{1-x}Cu_xCo_2O_4$ ($0 \le x \le 0.75$) electrodes the dominant component seems to be the surface composition, while for $NiCo_{2-y}Cu_yO_4$ ($0 \le y \le 0.30$) the real surface area plays an important role.

Conclusion

The study of the oxide spinel systems with nominal compositions $Ni_{1-x}Cu_xCo_2O_4$ and $NiCo_{2-y}Cu_yO_4$ led us to conclude that the differences in the electrochemical behaviour shown by the two systems reflect the use of different procedures in the electrodes' preparation.

Changes in the electrochemical behaviour are also caused by the presence of copper, because it induces modifications in the cationic distribution and consequently in the electrode surface composition, which the different limit of the solid solution formation and the non-variation of the lattice parameter suggest. These aspects are more evident in the system where copper replaces nickel.

The oxygen evolution efficiency determined in terms of overpotential depends on the electrodes' real surface area and follows the $(Ni/Co)_{XPS}$ variation, increasing with the increase of nickel content on the electrode surface.

Acknowledgements Financial support of the programme PRAXIS XXI (Proj. 435 PRAXIS/PCEX/C/QUI/83/96) from the Ministério da Ciência e Tecnologia is acknowledged. A.C.T. also acknowledges a PRAXIS XXI/BD/2648/93 grant.

References

1. Hanen J, Wisscher W, Barendrecht E (1986) J Electroanal Chem 208: 273
2. Rasiyah P, Tseung ACC (1982) J Electrochem Soc 129: 1724
3. Tavares AC, da Silva Pereira MI, Mendonça MH, Nunes MR, da Costa FMA, Sá CM (1998) J Electroanal Chem 449: 91
4. da Silva Pereira MI, da Costa FMA, Tavares AC (1994) Electrochim Acta 39: 1571
5. Gautier JL, Trollund E, Rios E, Nkeng P, Poillerat G (1997) J Electroanal Chem 428: 47
6. Schannon RD (1976) Acta Crystallogr A32: 751
7. Tavares AC, Cartaxo MAM, da Silva Pereira MI, da Costa FMA (1999) J Electroanal Chem 464: 187
8. Carapuça HMCS, Pereira MIS, da Costa FMA (1990) Mater Res Bull 25: 1183
9. Briggs D, Seah MP (1990) Practical surface analysis, vol 1. Wiley, Chichester, pp 223, 572–588
10. Adem E (1991) XPS and Auger handbook. Fisons Instruments Surface Science, Loughborough, UK
11. JCPDS (1988) Powder diffraction file 20–181. International Center for Diffraction Data, Swarthmore, USA
12. JCPDS (1988) Powder diffraction file 5–661. International Center for Diffraction Data, Swarthmore, USA
13. JCPDS (1988) Powder diffraction file 4–835. International Center for Diffraction Data, Swarthmore, USA
14. Tavares AC (1998) Tese de Doutoramento. Universidade de Lisboa
15. Appleman DE, Evans HT (1973) Indexing and least squares refinement of powder diffration data, report USG-GD-73-003. US Geological Survey, Washington DC
16. Haber J, Stoch J, Ungier L (1976) J Electron Spectrosc Relat Phenom 9: 439
17. McIntyre NS, Cook MG (1975) Anal Chem 47: 2208
18. Yin L, Adler I, Tsang T, Matienzo LJ, Grim SO (1974) Chem Phys Lett 24: 81
19. Kim KS, Davis RE (1972/73) J Electron Spectrosc Relat Phenom 1: 251
20. Kim KS, Winograd N (1974) Surf Sci 43: 625
21. Brundle CR, Carley AF (1975) Chem Phys Lett 31: 423
22. Roginskaya YE, Morozova OV, Lubnin EN, Ulitina YE, Lopukhova GV, Trasatti S (1997) Langmuir 13: 4621
23. Ikeo N (1991) Handbook of X-ray photoelectron spectroscopy. JEOL, Akishima, Japan
24. Klissurski D, Uzumova E (1992) J Mater Chem 2: 9653
25. Hanen J, Wisscher W, Barendrecht E (1986) J Electroanal Chem 208: 323

26. Blasse G (1963) Philips Res Rev 18: 383
27. Knop O, Reid KIG, Sutarno, Nakagawa Y (1968) Can J Chem 46: 3463
28. Hamdani M, Koenig JK, Chartier P (1988) J Appl Electrochem 18: 568
29. McLure DS (1957) J Phys Chem Solids 3: 311
30. Petrov K, Karamaneva T, Angelov S, Mehandjev D (1983) Mat Res Bull 18: 673
31. Baussart H, Dehobel R, Le bras M, Leroy JM (1979) J Chem Soc Faraday Trans 1 75: 1337
32. Kester E, Gillot B, Perriat P, Dufour P, Villette C, Tailhades P, Rousset A (1996) J Solid State Chem 126: 7
33. Fradette N, Marsain B (1998) J Electrochem Soc 145: 2320
34. Pourbaix M (1966) Atlas of electrochemical equilibria in aqueous solutions. Pergamon Press, Oxford
35. Marsain B, Fradette N, Beaudoin G (1992) J Electrochem Soc 139: 315
36. Nikolov I, Darkaoui R, Zhecheva E, Stoyanova R, Dimitrov N, Vitanov T (1997) J Electroanal Chem 429: 157
37. Trasatti S (1994) Transition metal oxides: versatile materials for electrocatalysis. In: Lipkowski J, Ross PN (eds) Electrochemistry of novel materials-frontiers of electrochemistry. VCH, New York, p 207
38. Hu CC, Lee YS, Wen TC (1997) Mat Chem Phys 48: 246
39. Tavares AC, Bochatay L, da Silva Pereira MI, da Costa FM (1996) Electrochim Acta 41: 1953
40. Trasatti S, Lodi G (1981) Oxygen and chlorine evolution reactions on conductive metallic oxide anodes. In: Trasatti S (ed) Electrodes of conductive metallic oxides, part B. (Studies in physical and theoretical chemistry, vol 11) Elsevier, Amsterdam, p 522